

Research article

Land Surface Temperature Retrieval from Landsat 9 Satellite Data in the Case of Injibara Town and the Surrounding Banja District, Awi Nationality Administrative Zone, Amhara, Ethiopia

Minyichil Teshome Kassahun*, Nigatu Amsalu Workineh

Injibara University, Department of Land Administration and Surveying, Injibara, Ethiopia.

*) Correspondence: minyt23@gmail.com

Citation:

Kassahun, M.T., & Workineh, N. A. (2025). Land Surface Temperature Retrieval from Landsat 9 Satellite Data in the Case of Injibara Town and the Surrounding Banja District, Awi Nationality Administrative Zone, Amhara, Ethiopia. Forum Geografi. 39(2), 125-135.

Article history:

Received: 18 October 2024 Revised: 15 May 2025 Accepted: 17 June 2025 Published: 26 July 2025

Abstract

Land surface temperature (LST) is crucial for various applications like agriculture, hydrology, urban planning, and climate analysis. Rapid urbanization and climate change have intensified LST variations, particularly in agriculturally dependent regions like Ethiopia, where temperature fluctuations directly impact livelihoods. However, localized LST dynamics in areas such as Injibara town and Banja District remain understudied, despite their sensitivity to climate variability and urban heat effects. This study addresses the gap by estimating LST using Landsat 9 data and analyzing its correlation with Normalized Difference Vegetation Index (NDVI). Landsat 9, launched in 2021, provides enhanced imaging capabilities and advanced sensors compared to its predecessors. Data from the United States Geological Survey (USGS) Earth Explorer website were processed using ArcGIS 10.8. LST was derived using the emissivity equation model incorporating land surface emissivity (LSE) and brightness temperature calculations. NDVI analysis revealed values ranging from -0.03 to 1, with high vegetation (0.35 - 1) concentrated in government and private forests in the northwest, while low vegetation (-0.03-0.15) dominated urban areas, barren lands, and unproductive regions in the south and southeast. The LST results indicated the highest temperatures (38-43°C) were in the northwest and southeast lowland regions, while the lowest temperatures (14-22°C) were in the central highlands. Approximately 40.8% of the area exhibited temperatures between 29-32°C. The study result revealed a negative relationship (R²=0.2506) between LST and NDVI, indicating that higher vegetation cover is associated with lower temperatures. To support regional climate resilience, we recommend integrating green infrastructure in urban planning, prioritizing afforestation in Banja's lowlands, and expanding research to other Ethiopian agro-ecological zones using high spatial resolution data for comparative analysis.

Keywords: correlation; Lake Zengena; land surface emissivity; operational land imagery; thermal infrared sensor.

1. Introduction

Urbanization is the intensification of inner-city inhabitants and urban land cover expansion due to the relocation of people into urban regions and the transformation of rural spaces into urban areas. By 2050, it is projected that 68% of the world's population will reside in urban areas, with global urban land area expected to continue expanding rapidly (United Nations, 2018; Chen *et al.*, 2020). The rise in land surface temperature is primarily driven by unplanned rapid urban development. Urban expansion and built-up areas contribute to an increase in land surface temperature (Rahaman *et al.*, 2023). Therefore, the urban population will be exposed to climate change risks from the rise in urban land surface temperature (Vohra *et al.*, 2024).

In today's world, climate change is one of the most pressing challenges we face. Land surface temperature (LST) is a crucial factor in understanding climate change and its effects (Li *et al.*, 2022). It is also a significant parameter for a variety of applications, such as agriculture, hydrology, and urban planning (Ghasempour *et al.*, 2023). In the past, LST was estimated using interpolation after the calculation of particular sample points. However, with the advent of earth observation satellites, LST is now routinely estimated using remote sensing data, which offers global spatial coverage, long-term records, and high spatiotemporal resolution (Zhang *et al.*, 2021). Thus, LST can be obtained and used easily for environmental monitoring and management. Landsat 9 was successfully launched in September 2021. Like Landsat 8, it supersedes previous Landsat generations in both radiometric and geometric measurements, in addition to its high imaging capacity (NASA, 2021). Moreover, Landsat 9 confirmed greater accuracy in land surface temperature analysis in addition to being equipped with advanced OLI and TIRS sensors compared to Landsat 8 and other previous Landsat satellites (Ghasempour *et al.*, 2023).

When compared to other satellite systems with thermal sensors, such as MODIS (Moderate Resolution Imaging Spectroradiometer) and Sentinel-3's SLSTR (Sea and Land Surface Temperature Radiometer), Landsat 9 stands out for its higher spatial resolution. While MODIS offers daily global coverage with a spatial resolution of 1 km for thermal bands (Zhang *et al.*, 2021; NASA, 2022), Landsat 9 provides finer thermal imagery at 100 m resolution, making it more suitable for



Copyright: © 2025 by the authors. Submitted for possible open access publication under the terms and conditions of the Creative Commons Attribution (CC BY) license (https://creativecommons.org/licenses/by/4.0/).

localized studies. On the other hand, Sentinel-3, with a resolution of 1km in thermal bands (ESA, 2013), surpasses Landsat 9 in terms of frequent revisits but lacks the spatial detail provided by Landsat 9. This balance of high spatial resolution and improved radiometric accuracy positions Landsat 9 as a crucial tool for detailed surface temperature studies, complementing broader datasets from other satellites.

Various studies have explored LST from diverse perspectives globally and to some extent in Ethiopia. For instance, Fikriyah *et al.* (2022) investigated the impact of built-up areas on urban LST using Landsat data in Surakarta, Indonesia, revealing the significant influence of urban structures on temperature variations. Similarly, Li *et al.* (2022) examined the relationship between urban expansion and the urban heat island effect in Surakarta, highlighting a positive correlation between urbanization and LST. In the context of Africa, Li *et al.* (2022) explored urbanization and climate change impacts on thermal urban environments, emphasizing the challenges posed by urban heat islands in rapidly urbanizing areas.

In Ethiopia, Yeneneh *et al.* (2022) studied the relationship between land use/land cover (LULC) changes and LST in the northwestern highlands, demonstrating how changes in vegetation and urban development influence thermal patterns. Similarly, Worku *et al.* (2021) analyzed the effects of vegetation cover change on LST in Addis Ababa, underscoring the critical role of green spaces in regulating urban temperatures. Earlier research by Damite (2017) focused on land surface change estimation in Bahir Dar city, providing valuable insights into urban expansion and its thermal implications.

This study distinguishes itself from previous research by its method, objectives, and the agroecological zone of the study area, which focuses on estimating LST in and around urban towns, incorporating both urban and surrounding rural environments. This approach allows for a comprehensive understanding of the interactions between urbanization and LST beyond urban boundaries. For instance, the research methodology combines the emissivity equation model (Rahaman *et al.*, 2023) with NDVI-based emissivity correction, addressing limitations of prior studies in Ethiopia that used simpler split-window algorithms (Damtie, 2017).

Furthermore, the study area encompasses two distinct climatic regions of Ethiopia, the highlands (Dega) and dry humid regions, enabling an analysis of the relationship between NDVI (Normalized Difference Vegetation Index) and LST across varying climatic conditions. By addressing these unique aspects, this research contributes to the broader understanding of LST dynamics in diverse agro-ecological zones.

This research aims to estimate the LST of the study area and examine the relationship between NDVI and LST using Landsat 9 satellite images for the year 2023, focusing on Injibara town and the surrounding Banja district, Ethiopia. This region was chosen due to its sensitivity to climate variability, being a predominantly agricultural area where temperature changes directly impact crop productivity and local livelihoods. Moreover, rapid urbanization in Injibara town has raised concerns about urban heat island effects and their implications for regional climate and human comfort. By enhancing the understanding of LST in and around the research area, this study aims to support climate change studies and provide a basis for developing sustainable land management and urban planning strategies. Additionally, this research seeks to address the knowledge gap on current LST patterns in the region. It also aims to understand the relationship between LST and NDVI in different Ethiopian climate regions, serve as a reference for similar studies, and inspire further research on climate change impacts in Ethiopia.

This paper is structured as follows: Section two reviews LST retrieval techniques and regional studies; Section three details the study area and methodology; Section four presents NDVI and LST results; Section five discusses spatial patterns and their implications; and Section six concludes with policy recommendations and future research directions.

2. Literature Review

2.1. Remote Sensing and Land Surface Temperature (LST)

LST is a critical parameter in understanding climate dynamics, urban heat island effects, and environmental monitoring. It both influences and is influenced by various atmospheric processes and surface properties. The advent of remote sensing technology, primarily through satellites like Landsat, has revolutionized the measurement and analysis of LST by providing consistent, high-resolution, and large-scale data (Ghasempour *et al.*, 2023). Landsat satellites, operated by the National Aeronautics and Space Administration (NASA) and the US Geological Survey, have been instrumental in earth observation since 1972. Each generation of Landsat satellites has brought improvements in sensor technology and data accuracy. Landsat 8, launched in 2013, introduced

Operational Land Imagery (OLI) and Thermal Infrared Sensor (TIRS), enhancing LST retrieval capabilities (Wang *et al.*, <u>2019</u>). The most recent addition, Landsat 9, launched in 2021, builds on these advancements with superior radiometric and geometric performance, further refining LST analysis (NASA, <u>2021</u>; Ghasempour *et al.*, <u>2023</u>).

2.2. LST Estimation Techniques

While various LST estimation techniques exist, each presents inherent limitations. The Split Window Algorithm (SWA), though effective for atmospheric correction, requires two thermal bands and may perform suboptimally in dry atmospheric conditions (Li *et al.*, 2023). Single-channel methods are more straightforward but often lack comprehensive atmospheric compensation, potentially reducing accuracy in heterogeneous environments (Mustafa *et al.*, 2020).

Recent advancements in satellite technology, particularly with the Landsat 9 TIRS-2 sensor, offer improved radiometric performance and atmospheric penetration, enhancing the reliability of LST retrieval. Moreover, integrating NDVI-based emissivity correction has become a widely recommended approach to account for land cover variability and further improve the accuracy of LST estimates (Ghasempour *et al.*, 2023). This study addresses the abovementioned gaps by leveraging the advanced capabilities of Landsat 9 and incorporating NDVI-based emissivity

2.3. Importance of Normalized Difference Vegetation Index (NDVI)

The Normalized Difference Vegetation Index (NDVI) is a commonly used measure in remote sensing to evaluate vegetation coverage. It is derived from the near-infrared and visible light that vegetation reflects and is indicative of plant health, biomass, and coverage (Rahaman *et al.*, 2023). NDVI is crucial in LST studies as vegetation cover significantly influences surface temperature. Areas with high NDVI values typically exhibit lower LST due to evapotranspiration and shading effects, while regions with low NDVI values tend to have higher LST (Ma *et al.*, 2022).

2.4. Regional Studies and Their Findings

While extensive research has been conducted globally, studies focusing on Ethiopia are limited. Damite (2017) explored LST using Landsat data in Bahir Dar Zuria, highlighting how changes in land cover affect surface temperatures. Similar studies in other African regions have shown that remote sensing is an effective technology for LST estimation and its relevance for urban planning and climate resilience (Syawalina *et al.*, 2022).

It can be concluded that incorporating remote sensing technologies such as Landsat 9 for estimating LST offers valuable insights into environmental and climatic dynamics. By understanding the relationship between LST and NDVI, we can more effectively evaluate the effects of urban expansion that leads to urbanization and land cover changes on local climates. This literature review highlights the necessity of ongoing research and technological advancements in remote sensing for efficient environmental protection and control.

3. Materials and Methods

3.1. Description of the Study Area

The research was conducted in Injibara town and the surrounding area of Banja district, which is located in the Amhara region of the Awi Nationality Zone Administration, Ethiopia. Injibara town is one of the leading fast-developing towns in the Amhara region. It is the center of the Awi Nationality Administrative Zone. Geographically, Injibara town and the surrounding Banja district are located in a latitude of between 100° 40′ 00″ N and 110° 10′00″ N and a longitude of between 36°40′ 00″ E and 37° 10′ 00″ E, as shown in Figure 1.

The study area exhibits significant topographic variation, with elevations ranging from a minimum of 1,805 meters to a maximum of 2,835 meters, as depicted in Figure 2. A substantial portion of the area lies within the elevation range of 2,451 to 2,579 meters above mean sea level. Within this context, Injibara town is situated at an altitude of 2,540 meters above sea level, with an average temperature of 15°C. Additionally, Injibara and its surroundings experience an average annual rainfall ranging from 700 to 2,500 mm. In contrast, the nearby Banja district, based on data from the Banja Woreda Agricultural Office, has an average annual temperature of 25°C, with recorded extremes of 16°C (minimum) and 30°C (maximum). The district receives an annual rainfall between 2,200 and 2,400 mm, which is favorable for agricultural activities. According to Ethiopia's climatic classification, Injibara town falls within the highland (Dega) zone, while the surrounding Banja district is characterized as dry and humid.

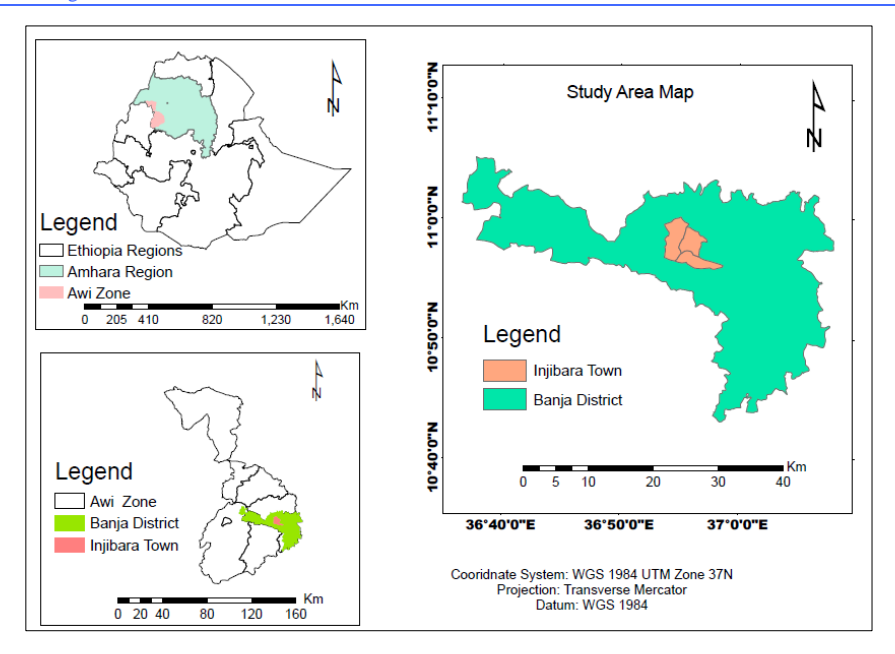


Figure 1. Study Area Map.

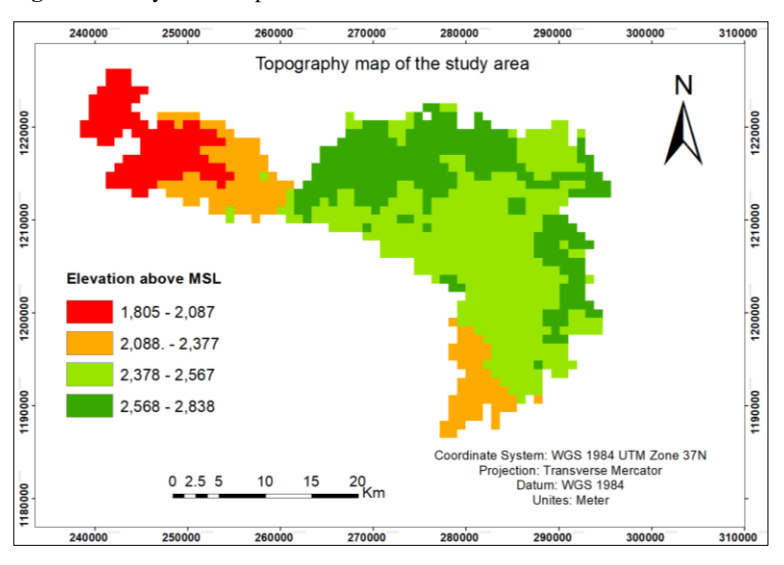


Figure 2. Topography map of the study area (Analyzed from ASTER DEM data).

3.2. Sources of Data

Remote sensing is a powerful technology providing updated data for the study of climate, hydrologic, ecological, and biogeochemical issues. Remote sensing data, which is satellite images, can be accessed freely from the USGS Earth Explorer. In this study, we utilized Landsat 9 Collection 2 Level-1 data, a standard product provided by the United States Geological Survey (USGS) for the year 2023, to understand the current LST of Injibara town and the surrounding Banja district. This level of data undergoes radiometric calibration and geometric correction to ensure accurate reflectance values and spatial consistency. Radiometric corrections account for sensor calibration and atmospheric effects, while geometric corrections align the data with a global reference system. Additionally, systematic terrain corrections, based on a Digital Elevation Model, are applied to mitigate distortions caused by Earth's topography, ensuring high spatial accuracy. The data are provided in the Universal Transverse Mercator (UTM) projection using the World Geodetic System 1984 (WGS84) datum. For land surface temperature (LST) retrieval, we specifically employed the thermal infrared sensor (TIRS) bands, which provide top-of-atmosphere (TOA) brightness temperatures critical for LST calculations. Landsat 9 products in Landsat Collection 2 Level-1 are processed using the Landsat Product Generation System (LPGS). This processing ensures that the thermal infrared sensor (TIRS) bands are resampled to a spatial resolution of 30 meters, aligning with the resolution of the multispectral bands. This resampling is essential for maintaining consistency between the thermal and multispectral data, enabling accurate integration and analysis for applications such as land surface temperature (LST) retrieval (EROS, 2020). The data details are presented in Table 1.

Table 1. Description of the Landsat 9 satellite image.

Acquisition date	Sensor	Path	Row	Band	Resolution
10/2/2023	OLI	170	052	1-9	30m
10/2/2023	TIRS	170	052	10&11	30m

Table 2. Details the values of thermal constant in Landsat 9 from metadata.

Constant value	Band 10	Band 11
K1	774.8853	475.6581
K2	1321.079	1198.349

Table 3. Rescaling factor of Landsat 9 from metadata.

Rescaling factor	Band 10	Band 11
ML	0.0004	0.00035
AL	0.1	0.1

3.3. Procedure of the study

Figure 3 illustrates the workflow used for land surface temperature (LST) retrieval and analysis from Landsat 9 satellite imagery. The process begins with the acquisition of Landsat 9 satellite images, specifically utilizing bands 4 (Red), 5 (Near Infrared, NIR), 10, and 11 (Thermal Infrared, TIR). Bands 4 and 5 are used to compute the Normalized Difference Vegetation Index (NDVI), which quantifies vegetation cover in the study area. The NDVI values are then used to calculate the proportion of vegetation (PV), an important parameter for estimating land surface emissivity (LSE).

Simultaneously, bands 10 and 11, which capture thermal infrared data, are processed by converting the digital numbers (DN) to spectral radiance. The spectral radiance values are then transformed into brightness temperature. Using the calculated LSE and brightness temperature, LST is estimated for both bands 10 and 11. The mean LST is then computed to represent the final land surface temperature for each pixel. Finally, a correlation analysis is conducted between the derived NDVI and LST values to examine the relationship between vegetation cover and land surface temperature in Injibara town and the surrounding Banja District. This methodological framework ensures accurate retrieval and analysis of LST, providing valuable insights into the spatial patterns of urban heat and vegetation dynamics in the study area.

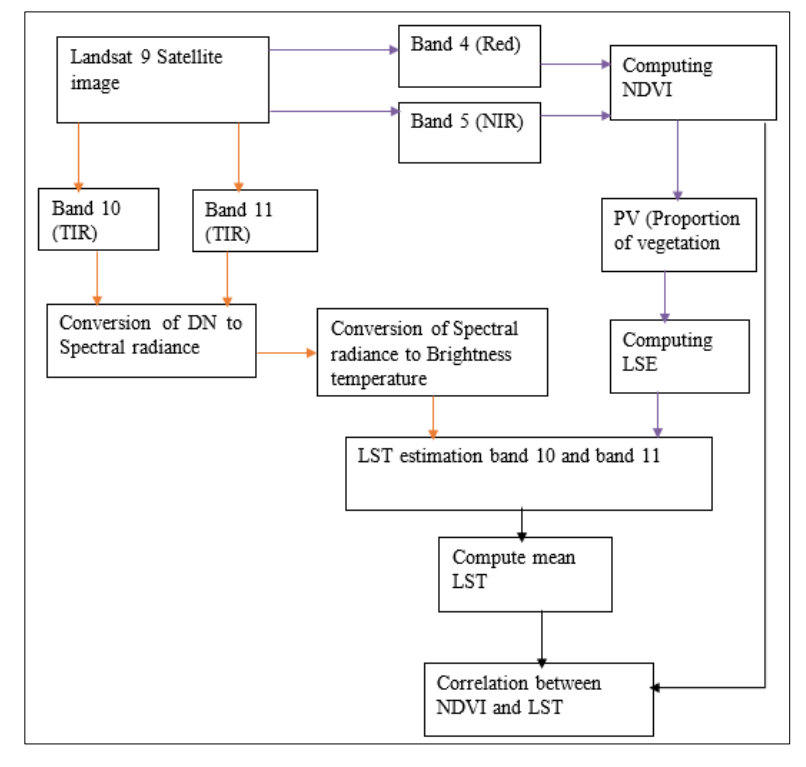


Figure 3. Working flowchart.

3.3.1. Data processing

As shown in the flow chart above, the first step to calculate LST is downloading the required data. The data was then processed using the appropriate software, ArcGIS 10.8. LST estimation using Landsat data was based on the following basic stages.

1. Compute Top of Atmosphere Radiance (TOA): Thermal infrared digital numbers are converted to top-of-atmosphere (TOA) radiance using the radiance rescaling factor from the metadata, as outlined in Equation 1 (Singh & Singla, 2024).

$$L\lambda = ML * Ocal + AL \tag{1}$$

Where $L\lambda$ represents the top-of-atmosphere (TOA) spectral radiance in units of Watts per square meter per steradian per micrometer (W/ (m² * sr * μ m)), ML refers to the radiance multiplicative band number, AL is the radiance additive band number, and Qcal denotes the quantized and calibrated pixel values from the standard product, measured in digital numbers.

2. Convert Top of Atmospheric Radiance to Top of Atmospheric Brightness (TOB) using K₁ and K₂ constant bands from metadata in Equation 2 (Reddy & Manikiam, 2017).

$$BT = \frac{k_2}{\ln\left(\left(\frac{k_1}{L\lambda}\right) + 1\right)} - 273.15 \tag{2}$$

Where BT represents the atmosphere brightness temperature at the satellite (°C), L λ is the TOA spectral radiance (Watts/ (m² * sr * μ m)), and K₁ and K₂ are the thermal fixed values of the bands (No.).

3. NDVI (Normalized Difference Vegetation Index) is an important factor in estimating LST by identifying long-term variation in vegetation coverage. It can be calculated by using near-infrared and red bands in Equation 3.

$$NDVI = \frac{(NIR - RED)}{(NIR + RED)}$$
(3)

Where RED is the Digital Number value of band 4, and NIR is the Digital Number value of Band 5.

According to Wahyunto (2006), NDVIs are classified into five classes, ranging from NDVI between -1 and -0.03, -0.03 and 0.15, 0.15 and 0.25, 0.25 and 0.35, and 0.35 and 1, with non-vegetation land-cover, very low vegetation land-cover, low vegetation land, medium vegetation land, and high vegetation land, respectively.

4. Compute the Land Surface Emissivity. It represents the emissive power of the Earth's component over a specific area on the Earth's surface and is determined by examining normalized difference vegetation index data using Equation 4 (Singh & Singla, 2024).

$$PV = \left[\frac{(NDVI - NDVI \, min)}{(NDVI \, max - NDVI \, min)} \right]^2 \tag{4}$$

Where PV is the proportion of vegetation, NDVI is the DN value of the normalized vegetation index, and NDVI min and NDVI max are the minimum and maximum DN values of the normalized vegetation index (Equation 5).

$$\varepsilon = u * pv + r \tag{5}$$

 ε is Land Surface Emissivity, PV is Proportion of Vegetation, u = 0.004, and r = 0.986

5. Calculate the LST. It represents the average temperature of an object on the Earth's surface. It is determined by calculating the emitted wavelength vivacity, the brightness temperature at the top of the atmosphere, and the land surface emissivity, as of Equation 6 (Avdan & Jovanovska, 2016; Reddy & Manikiam, 2017).

$$LST = \frac{BT}{\{1 + \left[\left(\lambda * \frac{BT}{14388}\right) * ln(\varepsilon)\right]\}}$$
(6)

Where BT represents the atmosphere brightness temperature at the satellite in ${}^{\circ}$ C, λ represents the wavelength of released vivacity, ϵ is the land surface emissivity, and 14388 is a value derived from the emissivity of the black body.

6. Correlation between NDVI and LST. NDVI is a measure of vegetation greenness, while LST is a measure of the surface temperature of the Earth. Therefore, understanding the correlation between NDVI and LST is very important for climate change. For this study, the correlation between them is analyzed using a linear regression equation in Equation 7.

$$Y = mx + b \tag{7}$$

Where Y is the dependent variable (LST), x is the Independent variable (NDVI), b is the x-intercept, and m is the slope of the line.

4. Result

This section presents the main results of the estimated Land Surface Temperature and Normalized Difference Vegetation Index, along with their correlation, in Injibara town and the surrounding Banja district. Additionally, these results will discuss the values of NDVI and LST compared to other literature.

4.1. Normalized Difference Vegetation Index of Injibara Town and Surrounding Banja District

The NDVI results presented in Figure $\underline{4}$ describe NDVI values classified according to Wahyunto's ($\underline{2006}$) standards for February.

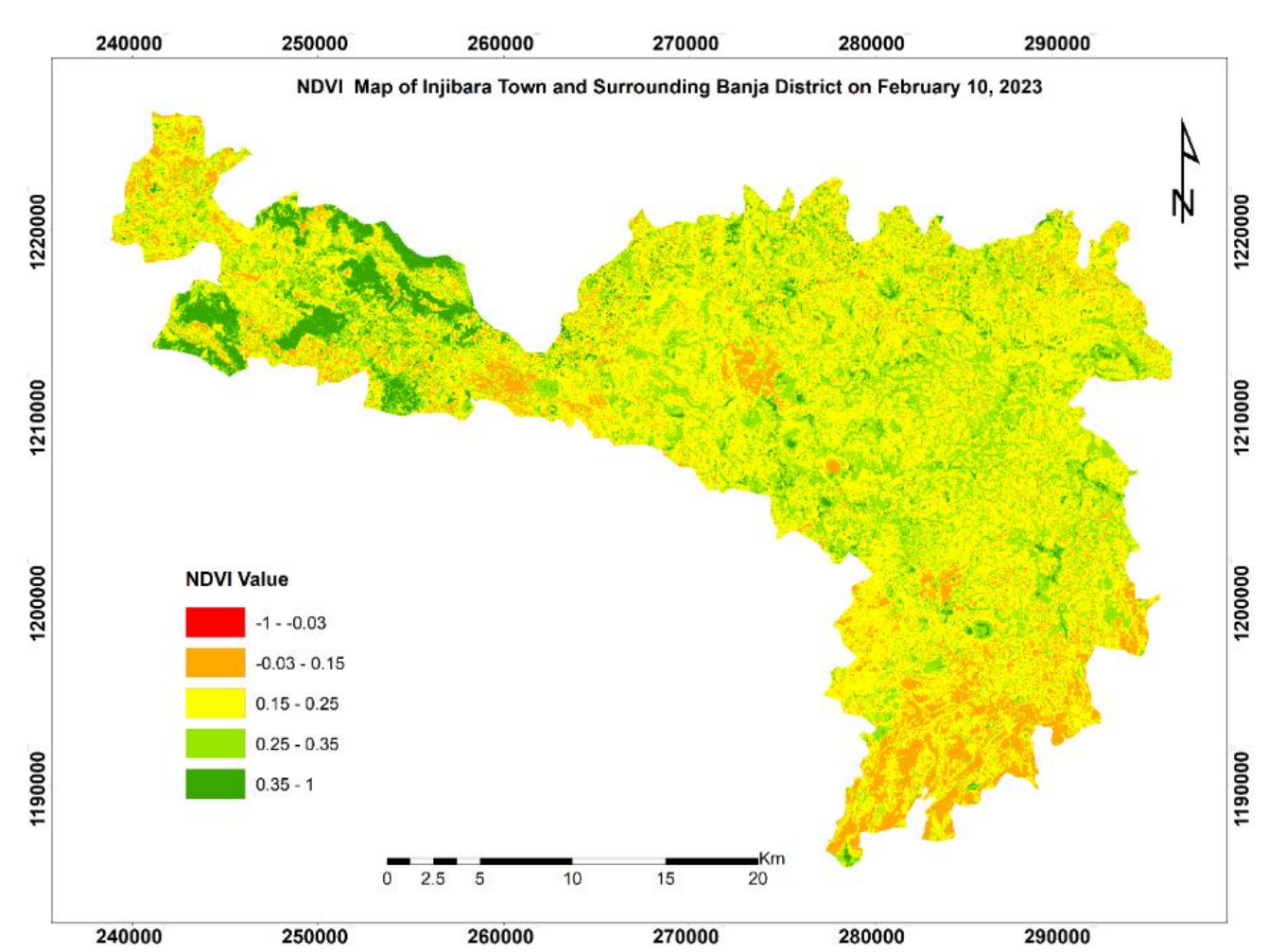


Figure 4. Classified NDVI map of Injibara Town and the Surrounding Banja District.

The analysis revealed significant spatial variations across the study area, with values ranging from -0.03 to 1, indicating a mix of sparse vegetation and moderately dense vegetation cover. Values ranging from 0.35 to 1 are observed in the northwest of the study area, primarily within government-owned forest areas. In contrast, values ranging from -0.03 to 0.15, indicating low vegetation cover, are detected in the central area, including Injibara town, Lake Zengena, developed lands such as roads and buildings, and in the southern to southeastern parts of the study area, which are characterized by barren and unproductive lands. A high spatial distribution is observed for NDVI values ranging from 0.15 to 0.25 across the study area.

4.2. Retrieved Land Surface Temperature of Injibara Town and Surrounding Banja District

The LST estimated, as from band 10 in addition to band 11 of the thermal infrared sensor on Landsat 9, is described in (Figure 5), depicts a minimum surface temperature of 14°C and a maximum surface temperature of 43 °C. The highest surface temperatures, ranging from 38 to 43°C, were observed in the Northwest and Southeast of the study area, where lowland areas and unproductive land were prevalent. The lowest surface temperatures, measured at 14–22 °C, were concentrated in the central highland area of the study region.

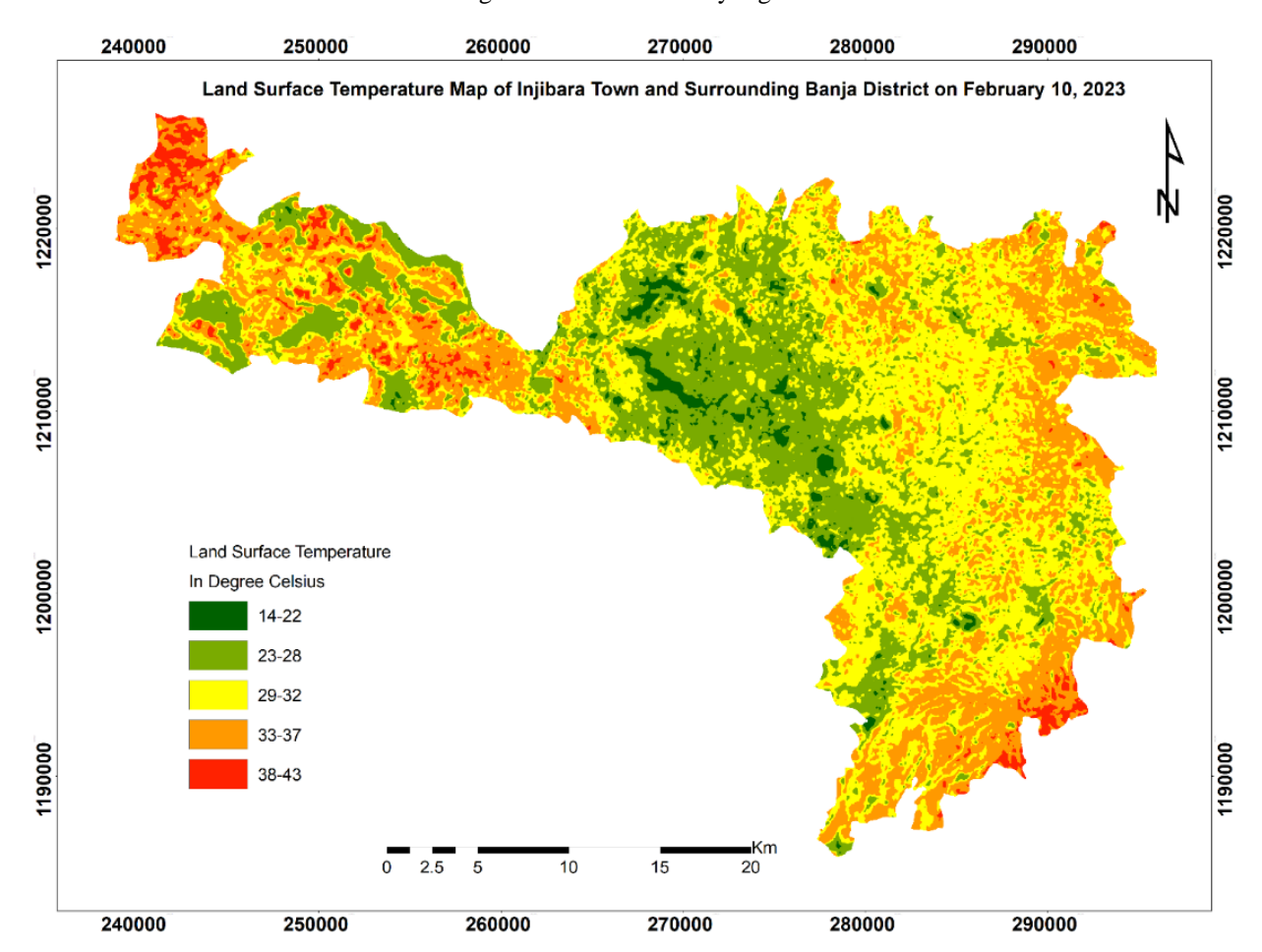


Figure 5. Map of retrieved LST in °C.

Out of the total 841.646 km² in the study area, 40% had an estimated temperature of 29-32°C, while 2.03% was covered by surface temperatures ranging from 14 to 22°C (Figure 6).

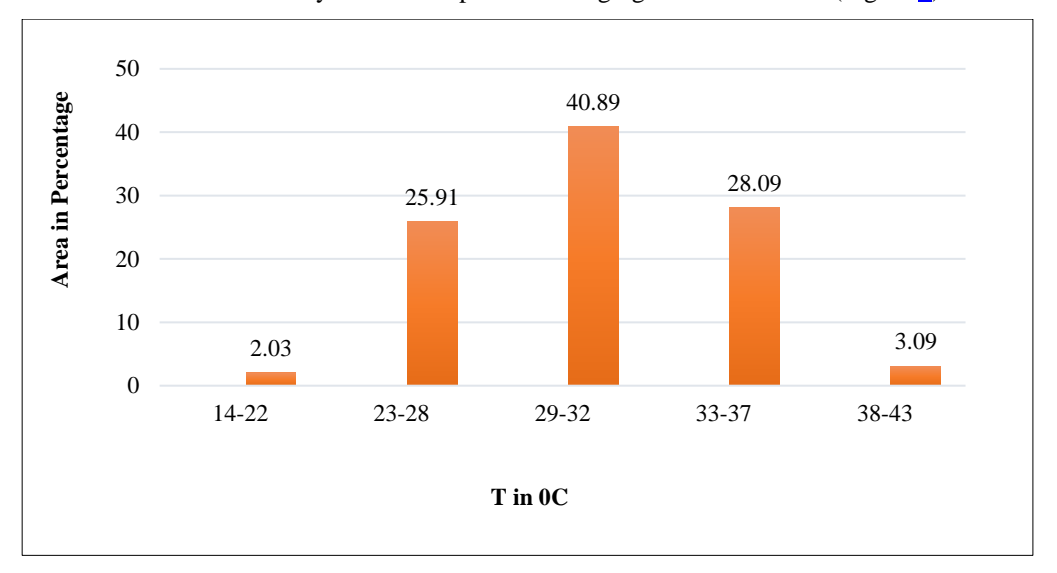


Figure 6. LST and area coverage in the study area.

4.3. Normalized Vegetation Index and Land Surface Temperature

Regression enquiry result indicated there is inverse relationship with land surface temperature and normalized difference vegetation index (Figure 7), the surface temperature for an NDVI range of 0.4 to 0.5 is between 20 and 24 °C, while for an NDVI range below 0.2, the surface temperature is between 25 and 41 °C.

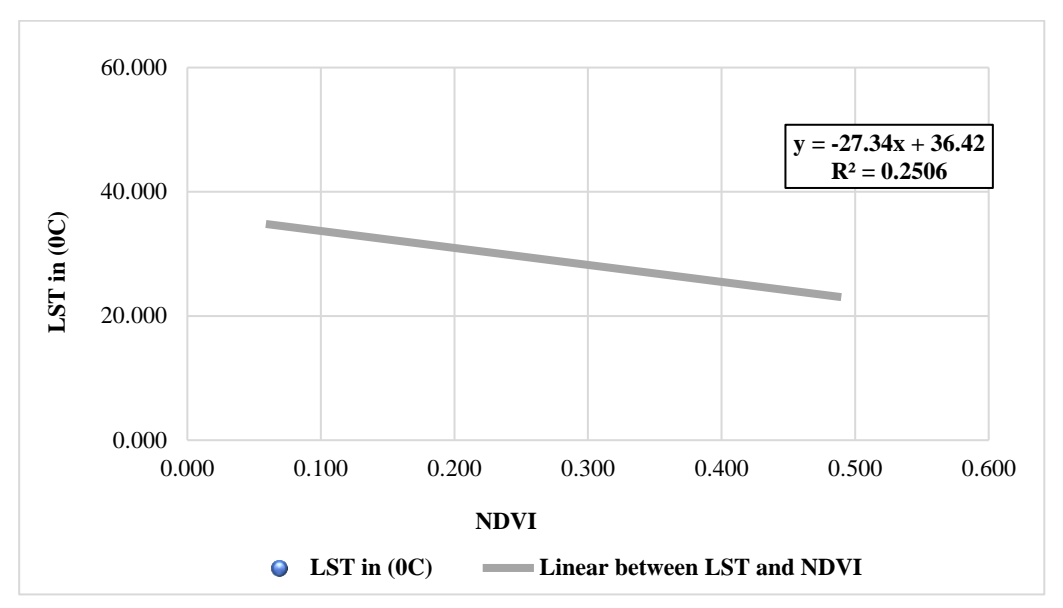


Figure 7. Relationship between LST and NDVI in degrees Celsius.

5. Discussion

The retrieval of LST from Landsat 9 thermal bands reveals a wide temperature range from 14°C to 43°C across Injibara town and the surrounding Banja District. This variation reflects the diverse land cover, elevation, and climatic conditions in the study area. Spatial analysis shows a clear correlation between LST and vegetation cover, as indicated by the NDVI patterns. Low vegetation areas, particularly in the southern and southeastern regions (e.g., latitude 11° 3′ 49″, longitude 36° 38′ 00′), exhibit the highest surface temperatures (38–43°C), dominated by barren land. This is consistent with recent findings, which highlight that barren and sparsely vegetated areas typically experience the highest temperatures due to reduced evapotranspiration and higher surface albedo. For example, a study in Rajkot, India, found that regions with barren land consistently exhibited higher LST, while areas with increased vegetation cover had lower surface temperatures. Similarly, recent analyses in Ernakulum District and other regions confirm a strong negative correlation between NDVI and LST, with vegetation cover acting as a key moderator of surface temperature extremes (Chen *et al.*, 2022).

Conversely, the cooler temperatures ($14-22^{\circ}C$) observed in highland areas with denser vegetation (e.g., latitude 10° 57' 09", longitude 36° 53' 09" in the northwest) underscore the influence of elevation and vegetation in mitigating surface heat. However, notable variations within the same NDVI range suggest that topography plays a critical role in LST distribution. For instance, at latitude 10° 57' 34" and longitude 36° 56' 05" (center of the study area) and latitude 10° 46' 46" and longitude 37° 3' 10" (southeast), areas with similar NDVI values exhibit contrasting LST ranges due to their differences in elevation. This highlights the complex interplay between vegetation, elevation, and land cover in shaping LST dynamics in Injibara and Banja District.

Urban areas in Injibara town reveal unique thermal characteristics compared to rural surroundings. Despite low vegetation cover, built-up areas in highland regions exhibited lower surface temperatures compared to lowland regions with barren or sparsely vegetated land. This underscores the role of elevation in moderating urban heat island effects, even in semi-arid settings. However, the moderately high temperatures (29–32 $^{\circ}$ C) prevalent across approximately 40% of the study area, particularly around latitude 10 $^{\circ}$ 54' 21" and longitude 36 $^{\circ}$ 54' 21", reflect the pervasive influence of semi-arid conditions and human activities, such as urban expansion and land degradation.

The regression analysis (Y = -27.34x + 36.42, $R^2 = 0.2506$) confirms a statistically significant inverse relationship between NDVI and LST. The R^2 value indicates that approximately 25% of the variation in LST can be explained by the variation in NDVI. Higher NDVI values (0.4–0.5) correspond to lower temperatures (20–24°C), whereas areas with NDVI values below 0.2 experience higher temperatures (25–41°C). This suggests that while vegetation cover plays a role in

influencing surface temperatures, other factors, such as elevation, soil moisture, and anthropogenic heat, also contribute to LST patterns in the study area. This finding aligns with previous studies that have reported a negative correlation between NDVI and LST (Maharani *et al.*, 2021; Rahaman *et al.*, 2023), further validating the role of vegetation in moderating surface temperatures. However, this study also reveals the importance of considering topographic variations, which can lead to deviations from this general trend.

Interestingly, the study also identifies instances where the inverse relationship between NDVI and LST is not strictly observed. Specifically, we found that some highland areas with low vegetation cover exhibit lower LST compared to lowland areas with relatively higher vegetation cover. This apparent anomaly underscores the significant influence of topography on thermal dynamics in the region. Higher elevations generally experience lower temperatures due to decreased air pressure and increased adiabatic cooling (Ma *et al.*, 2022). Recent studies confirm that elevation can be a dominant factor in controlling LST, sometimes overriding the effects of vegetation cover. For example, Rahaman *et al.* (2023) and Ma *et al.* (2022) both report that in mountainous or highland regions, LST is often more strongly correlated with elevation than with NDVI, due to the cooling effects associated with higher altitudes. Similarly, Chen *et al.* (2023) demonstrate that topographic variation significantly modulates LST patterns in complex terrain, highlighting that elevation-induced cooling can outweigh vegetation effects in specific contexts. These findings align with our results and emphasize the need to consider topography when interpreting LST-NDVI relationships in heterogeneous landscapes.

Injibara and Banja District face significant challenges due to extreme temperatures in lowland areas, raising concerns about the vulnerability of these zones to land degradation and climate change. These findings have critical implications for urban and rural planning. For Injibara, urban planners should prioritize integrating green infrastructure, such as urban forests and vegetative buffers, to mitigate urban heat island effects and enhance thermal comfort for residents. In the surrounding Banja District, afforestation and community-led forest conservation efforts are vital to reduce surface temperatures and combat land degradation.

The limitations of this research, which focuses on LST estimation from Landsat imagery for a single year, underscore the need for further studies. Temporal analysis over multiple years would provide a broader understanding of climatic and anthropogenic influences on LST and NDVI dynamics. Integrating socioeconomic data, such as population growth, land use changes, and economic activities, could offer valuable insights into the human dimensions of land degradation and temperature variation in the region. Moreover, refining the LST retrieval methodology to incorporate field-based validation would enhance the accuracy and applicability of remote sensing data for local decision-making.

This study demonstrates the potential of Landsat 9 data to effectively analyze LST and its drivers in diverse landscapes, such as Injibara town and Banja District. The findings highlight the critical role of vegetation, elevation, and urban planning in regulating surface temperatures and emphasize the need for sustainable land management strategies to address the challenges posed by rising temperatures and climate change.

6. Conclusion

This study successfully retrieved LST from Landsat 9 data using emissivity equations, calculated NDVI, and analyzed their correlation. The findings revealed that high vegetation areas, with NDVI values ranging from 0.4 to 0.5, exhibited low surface temperatures between 20°C and 24°C, while low vegetation areas, with NDVI values below 0.2, experienced higher surface temperatures ranging from 25°C to 41°C. The regression analysis (Y=-27.34x+36.42, R²=0.2506) confirmed an inverse correlation between NDVI and LST in the same topography, where areas with higher NDVI consistently corresponded to lower LST values. To support regional climate resilience, we recommend integrating green infrastructure in urban planning and prioritizing afforestation in Banja's lowlands. Future research should focus on expanding the analysis to other Ethiopian agroecological zones, incorporating higher spatial resolution thermal data sources where available, to validate and refine these findings across diverse environmental conditions.

Reference

Avdan, U., & Jovanovska, G. (2016). Algorithm for Automated Mapping of Land Surface Temperature using Landsat 8 Satellite Data. *Journal of Sensors*, 2016(1), 1480307.

Chen, M., Zhang, H., Liu, W., & Zhang, W. (2020). Global Projections of Future Urban Land Expansion Under Shared Socioeconomic Pathways. *Nature Communications*, 11, 537. doi: 10.1038/s41467-020-14386-x

Chen, J., Zhou, Y., Li, X., & Liu, X. (2023). Effects of Topography and Land Cover on Land Surface Temperature in Mountainous Regions. *Remote Sensing*, 15(4), 1056. doi: 10.3390/rs15041056

Acknowledgements

The authors would like to express their sincere gratitude to all parties who have contributed to the research and the completion of this manuscript. Special thanks are extended to mentors, funding institutions, and data providers for their invaluable support and assistance throughout the study.

Author Contributions

Conceptualization: Kassahun, M.T., & Workineh, N; methodology: Kassahun, M.T., & Workineh, N; investigation: Kassahun, M.T., & Workineh, N; writing—original draft preparation: Kassahun, M.T., & Workineh, N; writing—review and editing: Kassahun, M.T., & Workineh, N; visualization: Kassahun, M.T., & Workineh, N. All authors have read and agreed to the published version of the manuscript.

Conflict of interest

All authors declare that they have no conflicts of interest.

Data availability

Data is available upon Request.

Funding

This research received no external funding.

- Chen, S., Haase, D., Qureshi, S., & Firozjaei, M. K. (2022). Integrated Land Use and Urban Function Impacts on Land Surface Temperature: Implications for Urban Heat Mitigation in Berlin With Eight-Type Spaces. Sustainable Cities And Society, 83, 103944.
- Damtie, B. B. (2017). Estimation of Land Surface Temperature Using Landsat by Split Window Algorithm: A Case Study in Bahir Dar Zuria, Ethiopia. *J. Environ. Earth Sci.*, 7, 106-115.
- Earth Resources Observation and Science (EROS) Center. (2020). Landsat 8-9 Operational Land Imager / Thermal Infrared Sensor Level-1, Collection 2 [Dataset]. U.S. Geological Survey.
- ESA. (2013). Sentinel-3 GMES Medium Resolution Land and Ocean Mission. Retrieved From Http://Esamultimedia.Esa.Int/Docs/S3-Data_Sheet.Pdf
- Fikriya, V. N., Danardono, D., Sunariya, M. I. T., Cholil, M., Hafid, T. A., & Ismail, M. I. (2022). Spatio-Temporal Analysis of Built-Up Area and Land Surface Temperature in Surakarta Using Landsat Imageries. *Sustinere: Journal of Environment and Sustainability*, 6(2), 92-101.
- Ghasempour, F., Sekertekin, A., & Kutoglu, S. H. (2023). How Landsat 9 Is Superior to Landsat 8: Comparative Assessment of Land Use Land Cover Classification and Land Surface Temperature. ISPRS Annals of the Photogrammetry, Remote Sensing and Spatial Information Sciences, 10, 221-227.
- Ghasempour, V., Gholami, S., & Sharifi, A. (2023). Remote Sensing-Based Monitoring of Land Surface Temperature and Urban Heat Island: A Review of the State-of-the-Art and Future Perspectives. *Remote Sensing*, 15(3), 712. Doi: 10.3390/Rs15030712
- Li, X., Stringer, L. C., & Dallimer, M. (2022). The Impacts of Urbanization and Climate Change on the Urban Thermal Environment in Africa. *Climate*, 10(11), 164.
- Li, X., Zhou, Y., & Wang, Y. (2023). Advances in Land Surface Temperature Retrieval From Satellite Thermal Infrared Data: Methods and Applications. ISPRS Journal of Photogrammetry and Remote Sensing, 200, 1-19. Doi: 10.1016/J.Isprsjprs.2023.01.002
- Ma, Y., Zhao, Y., & Liu, Y. (2022). Spatiotemporal Analysis of the Relationship Between NDVI and Land Surface Temperature in Urban Areas. *Urban Climate*, 44, 101256. Doi: 10.1016/J.Uclim.2022.101256
- Maharani, A., Salsanur, V., Hilal, A., & Aprilian, Y. (2021). Preliminary Interpretation for Geothermal Potential Area Using DEM and Landsat OLI 8 in Mount Endut. *Bulletin of Scientific Contribution: Geology*, 19(1), 35-46.
- Mustafa, E. K., Co, Y., Liu, G., Kaloop, M. R., Beshr, A. A., Zarzoura, F., & Sadek, M. (2020). Study for Predicting Land Surface Temperature (LST) Using Landsat Data: A Comparison of Four Algorithms. Advances in Civil Engineering, 2020, 1-16.
- NASA. (2021). Landsat 9. Retrieved From Https://Landsat.Gsfc.Nasa.Gov/Satellites/Landsat-9/
- NASA. (2022). MODIS: An Overview. Retrieved From Https://Modis-Land.Gsfc.Nasa.Gov/
- Rahaman, K. R., Hassan, Q. K., & Ahmed, S. (2023). Assessment Of Land Surface Temperature And Its Relationship With NDVI Using Landsat Satellite Data: A Case Study From Bangladesh. *Environmental Challenges*, 10, 100689. Doi: 10.1016/J.Envc.2022.100689
- Reddy, S. N., & Manikiam, B. (2017). Land Surface Temperature Retrieval From LANDSAT Data Using Emissivity Estimation. *International Journal of Applied Engineering Research*, 12(20), 9679-9687.
- United Nations, Department of Economic and Social Affairs, Population Division (2018). World Urbanization Prospects: The 2018 Revision. Retrieved From Https://Population.Un.Org/Wup/Publications/
- Vohra, R., Kumar, A., Jain, R., & Hemanth, D. J. (2024). Analysis And Prediction of Land Surface Temperature with Increasing Urbanization using Satellite Imagery. Heliyon, 10(22).
- Rouse, J. W., Haas, R. H., Schell, J. A., & Deering, D. W. (1974). Monitoring Vegetation Systems in the Great Plains with ERTS. *NASA Special Publication*, 351, 309.
- Sekertekin, A., & Bonafoni, S. (2020). Land Surface Temperature Retrieval From Landsat 5, 7, And 8 Over Rural Areas: Assessment of Different Retrieval Algorithms and Emissivity Models and Toolbox Implementation. Remote Sensing, 12(2), 294.
- Singh, P., & Singla, S. (2024). Estimation of Land Surface Temperature of Srinagar City, India, Using Landsat 8 data. Sustainability, Agri, Food and Environmental Research, 12(1).
- Syawalina, R. K., Ratihmanjari, F., & Saputra, R. A. (2022). Identification Of The Relationship Between LST And NDVI on Geothermal Manifestations in a Preliminary Study of Geothermal Exploration Using Landsat 8 OLI/TIRS Imagery Data Capabilities: Case Study of Toro, Central Sulawesi. *Stanford University*, 1-8.
- Wahyunto. (2006). Land Cover Classification Standards in Tropical Regions. *International Journal of Remote Sensing*, 27(15-16), 3323-3332.
- Wang, M., Zhang, Z., Hu, T., & Liu, X. (2019). A Practical Single-Channel Algorithm for Land Surface Temperature Retrieval: Application to Landsat Series Data. *Journal Of Geophysical Research: Atmospheres*, 124(1), 299-316.
- Worku, G., Teferi, E., & Bantider, A. (2021). Assessing The Effects of Vegetation Change on Urban Land Surface Temperature Using Remote Sensing Data: The Case of Addis Ababa City, Ethiopia. Remote Sensing Applications: Society And Environment, 22, 100520.
- Yeneneh, Nigussie, Eyasu Elias, And Gudina Legese Feyisa. (2023). Detection Of Land Use/Land Cover and Land Surface Temperature Change in the Suha Watershed, North-Western Highlands of Ethiopia. Environmental Challenges 7, 100523.
- Zhang, T., Zhou, Y., Zhu, Z., Li, X., & Asrar, G. R. (2021). A Global Seamless 1 Km Resolution Daily Land Surface Temperature Dataset (2003–2020). Earth System Science Data Discussions, 2021, 1-16.